Vector Control and Direct Power Control of Wind Energy Conversion System based on a DFIG

SENANI Fawzi, RAHAB Abederrezak, BENALLA Hocine

Université des Frères Mentouri Constantine 1,
Laboratoire de l'Electrotechnique de Constantine (LEC), Faculté des Sciences de la Technologie,
Ain el-bey 25000 Constantine, Algérie, E-mail: senani.fouzi@gmail.com, rahab_abderezzak@yahoo.fr, benalladz@yahoo.fr

***Abstract* – The paper present the modeling and control of 1.5 MW wind energy conversion system (WECS) equipped with a DFIG for a variable speed. A bidirectional converter is employed for the power conversion exchanged between the machine stator and grid. The control strategy of DFIG and rotor side converter (RSC) combines the technique of MPPT included the control of the generator speed by Proportional Integral (PI) and vector control (VC). In the control system of the grid side converter (GSC) the application of direct power control (DPC) has been used. The results of simulation of the global control system have been presented and discussed.**

Keywords: ***WECS; MPPT; DFIG; VC DPC; PI controller.***

I. INTRODUCTION

In the past decades, a great increase in electrical power demand and depletion of natural resources have made environmental and energy crises [1], and especially after the oil crisis in the 1970s, global interest for clean and renewable energy sources has been growing intensively [2]. These have led to an increased need for production of energy from renewable sources so that [1], wind energy conversion (WEC) is the fastest-growing energy source among the new power generation sources in the world and this tendency should remain for some time due to cleanness and renewability [3].

Wind turbines which play a main role in wind energy, are basically divided into fixed and variable-speed technologies [1]. The latter are the most used for the production of electric power due to several advantages compared to fixed speed wind turbines. Indeed, variable speed wind turbines operate over a wide range of speeds, thus maximizing extracted power at low wind speeds and maintaining constant power at high wind speeds [4], decreased mechanical stresses imposed on the turbine, improved power quality, and decreased acoustical noise [1]. For the variable speed wind turbine, two types of generators are generally used: Doubly Fed Induction Generator (DFIG) with partial-scale converters and Permanent Magnet Synchronous Generator (PMSG) with full-scale converters [1, 2].

DFIG has become popular as a wind driven generator for high power applications due to the lower converters cost and lower power losses [1, 5], DFIG with fully controlled bidirectional converters rated at 25–30% of the generator rating for a given rotor speed variation range of ±25% and four quadrant active and reactive powers capabilities [1, 4, 5].

Control of DFIG based both the rotor side converter (RSC) and grid side converter (GSC) controllers so that the RSC controls stator active and reactive powers and the GSC regulates DC-link voltage as well as generates an independent reactive power that is injected into the grid [6], for RSC control the vector control (VC) based in flux oriented control is very attractive used wind turbine variable speed based in DFIG[7], this technique provides indirect control of active and reactive powers with proportional integral (PI) controllers [7, 8].

For the GSC control many works have been presented with different control techniques of pulse with modulation (PWM) rectifier associated with classical controllers [9]. Such as hysteresis band current control (HBCC) [10], voltage oriented control (VOC) [11], Therefore, different control methods are developed and proposed such as direct torque control (DTC) and direct power control (DPC) [12, 13]. DPC Based on the principles of DTC strategy proposed for three-phase PWM converters by [14] and developed later by [15].

This paper proposes a vector control (VC) of DFIG with RSC and direct power control (DPC) of GSC. The application of the MPPT to to extract the maximum converted power in addition the control of the generator speed by Proportional Integral regulator have been included.

II. WIND ENERGY CONVERSION CHAIN MODELING

The synoptic scheme WECS seen in Figure 1, composed: wind turbine connected to DFIG via a gearbox, two converters are insert between the rotor and the grid, the RSC operates to control a DFIG and the GSC is connected to the grid via a filter, a capacity energy storage system in the DC-link and the grid in which the electrical energy produced is injected [2, 9].

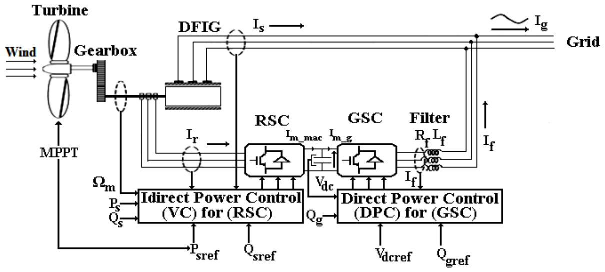

Fig. 1. Principle DFIG based wind energy conversion chain.

A. Wind turbine model

The available power of the wind crossing a surface S is defined by [16]:

$$P_v = \frac{1}{2}.\rho.S.v^3 \quad (1)$$

The aerodynamic power Pt captured by the wind turbine is given by [3, 17]

$$P_t = \frac{1}{2}.C_p(\lambda,\beta).\rho.S.v^3 \quad (2)$$

Cp is the power coefficient that characterizes the aerodynamic efficiency of the turbine. It is a function of the blade pitch angle β and the tip-speed ratio λ where λ is defined as [2, 3, 17]:

$$\lambda = \frac{\Omega_t.R}{v} \quad (3)$$

For a wind of 1.5 MW, the expression of the power coefficient can be approximated by [16, 18]:

$$C_p(\lambda,\beta) = \left(0.5 - 0.0167.(\beta-2)\right).sin\left[\frac{\pi.(\lambda+0.1)}{10-0.3.\beta}\right] - -0.00184.(\lambda-3).(\beta-2) \quad (4)$$

The aerodynamic torque expression [19]:

$$C_t = \frac{P_t}{\Omega_t} = \frac{\pi}{2.\lambda}\rho.R^3.C_p(\lambda,\beta) \quad (5)$$

The gearbox is the connection between the turbine and the generator to adapt the turbine speed to that of the generator. It is modeled by two equations [19]:

$$\Omega_m = G.\Omega_t \quad (6)$$

$$C_m = \frac{C_t}{G} \quad (7)$$

The mechanical equation of the wind turbine [19]:

$$J\frac{d\Omega_m}{dt} + f.\Omega_m = C_m - C_{em} \quad (8)$$

With: $J = \left(\frac{J_t}{G^2} + J_m\right)$

B. Modeling the DFIG

The electrical equations of the stator and rotor voltages of the DFIG in the Park model [18, 19]:

$$\begin{cases} V_{sd} = R_s I_{sd} + \frac{d\varphi_{sd}}{dt} - \omega_s\varphi_{sq} \\ V_{sq} = R_s I_{sq} + \frac{d\varphi_{sq}}{dt} + \omega_s\varphi_{sd} \end{cases} \quad (9)$$

$$\begin{cases} V_{rd} = R_r I_{rd} + \frac{d\varphi_{rd}}{dt} - \omega_r\varphi_{rq} \\ V_{rq} = R_r I_{rq} + \frac{d\varphi_{rq}}{dt} + \omega_r\varphi_{rd} \end{cases} \quad (10)$$

The flux equations of the DFIG given by [18, 19]:

$$\begin{cases} \varphi_{sd} = L_s I_{sd} + M I_{rd} \\ \varphi_{sq} = L_s I_{sq} + M I_{rq} \end{cases} \quad (11)$$

$$\begin{cases} \varphi_{rd} = L_r I_{rd} + M I_{sd} \\ \varphi_{rq} = L_s I_{rq} + M I_{rq} \end{cases} \quad (12)$$

d and q of the stator and rotor voltages, currents and flux.

The electromagnetic torque is expressed by:

$$C_{em} = p\frac{M}{L_s}\left(\varphi_{sd}I_{rq} - \varphi_{sq}I_{rd}\right) \quad (13)$$

The active and reactive power stator and rotor of the DFIG are given by:

$$\begin{cases} P_s = V_{sd}I_{sd} + V_{sq}I_{sq} \\ Q_s = V_{sq}I_{sd} - V_{sd}I_{sq} \end{cases} \quad (14)$$

$$\begin{cases} P_r = V_{rd}I_{rd} + V_{rq}I_{rq} \\ Q_r = V_{rq}I_{rd} - V_{rd}I_{rq} \end{cases} \quad (15)$$

C. Modeling of the grid side converter connection

The connection to the electrical grid constitutes the DC Link voltage, the GSC and the input filter R_fL_f.

1. DC Link voltage model

The voltage across the capacitor [19]:

$$\frac{dV_{dc}}{dt} = \frac{1}{C}.I_c \quad (16)$$

The current in the capacitor [19]:

$$I_c = I_{m\_grid} - I_{m\_mac} \quad (17)$$

$$V_s = V_g \quad (18)$$

2. Grid connect model

$$\begin{cases} V_{fa} = -R_s I_{fa} - L_f\frac{dI_{fa}}{dt} + V_{ga} \\ V_{fb} = -R_s I_{fb} - L_f\frac{dI_{fb}}{dt} + V_{gb} \\ V_{fc} = -R_s I_{fc} - L_f\frac{dI_{fc}}{dt} + V_{gc} \end{cases} \quad (19)$$

III. WIND ENERGY CONVERSION CHAIN CONTROL PROPOSED

To ensure the operation of the global wind turbine proposed three controls are detailed:

A. MPPT control

The electromagnetic torque Cem developed is equal to its reference value Cemref ($C_{emref} = C_{em}$) whatever the power generated if we assume that the generator is ideal [16, 19, 20].

This technique of extracting the maximum power consists in determining the speed of the turbine Ω_t which makes it possible to obtain the maximum power generated. Thus, the electromagnetic torque must be adjusted on the DFIG shaft so as to fix the rotational speed of the latter at a reference speed. Control of the speed of rotation of the DFIG must be achieved, as shown in Figure 2.

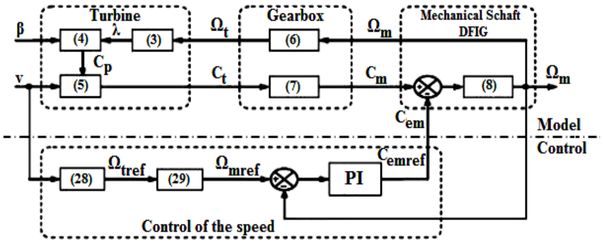

Fig. 2. Block diagram with speed control

The reference electromagnetic torque (C_{emref}) allowing it possible to obtain a rotational speed Ω_m equal to its reference value Ω_{mref} is obtained at the output of the speed regulator (Figure.2) [16, 19, 20]. In order to control the speed of rotation, we use Proportional Integral regulator (PI). The reference of the speed of the turbine (Ω_{tref}) corresponds to that of the optimum value of the tip-speed ratio (λ_{opt}) allowing it possible to obtain the maximum value of the C_{pmax}:

$$\Omega_{tref} = \frac{\lambda_{opt}.v}{R} \tag{20}$$

This reference speed (Ω_{mref}) depends on the speed of the turbine to fix Ω_{tref} for maximize the extracted power is given by:

$$\Omega_{mref} = G.\Omega_{tref} \tag{21}$$

B. *Indirect power control for RSC*

To do this, it is sufficient to orient the reference d, q so as to cancel the quadrature flux component. That is to say, to choose suitably the angle of rotation of Park so that the rotor flux is entirely aligned with the direct axis (d) and thus to have φ_{sq}=0, φ_{sd}= φ_s [2, 19]. In addition for medium and high power machines used in wind turbines, we can neglect the stator resistance while considering the constant stator flux [5, 21], and the grid is supposed stable with voltage V_s and synchronous angular frequency ω_s while considering the constant stator flux φ_{sd}=cst.

The expression of the electromagnetic torque:

$$C_{em} = p\frac{M}{L_s}I_{rq}\varphi_{sd} \tag{22}$$

The equations of DFIG in the d q reference:

$$\begin{cases} V_{sd} = \frac{d\varphi_{sd}}{dt} = 0 \\ V_{sq} = V_s = \omega_s\varphi_s \end{cases} \tag{23}$$

From equations of φ_{sd} and φ_{sq} in (11), the equations related the stator currents to the rotor currents:

$$\begin{cases} I_{sd} = -\frac{M}{L_s}I_{rd} + \frac{\varphi_s}{L_s} \\ I_{sq} = -\frac{M}{L_s}I_{rq} \end{cases} \tag{24}$$

According to equations (22) the stator active and reactive powers are written:

$$\begin{cases} P_s = V_sI_{sq} \\ Q_s = V_sI_{sd} \end{cases} \tag{25}$$

By replacing the stator currents of equations (23) in equations (24), we obtain the following expressions:

$$\begin{cases} P_s = -V_s\frac{M}{L_s}I_{rq} \\ Q_s = -V_s\frac{M}{L_s}I_{rd} + V_s\frac{\varphi_s}{L_s} \end{cases} \tag{26}$$

From equation (22), we have $\varphi_s = \frac{V_s}{\omega_s}$, the expression of reactive power becomes:

$$Q_s = -V_s\frac{M}{L_s}I_{rd} + \frac{V_s^2}{L_s\omega_s} \tag{27}$$

Moreover, the rotor voltages could be expressed as a function of the rotor currents, replacing the stator currents in equations φ_{rd} and φ_{rq} in (12), by the expressions (23).

$$\begin{cases} \varphi_{rd} = \left(L_r - \frac{M^2}{L_s}\right)I_{rd} + \frac{MV_s}{L_s\omega_s} \\ \varphi_{rq} = \left(L_r - \frac{M^2}{L_s}\right)I_{rq} \end{cases} \tag{28}$$

These expressions of the rotor fluxes of axis d and q are integrated in the expressions of the rotor voltages of equations V_{rd} and V_{rq} in (12), we then obtain:

$$\begin{cases} V_{rd} = R_rI_{rd} + \left(L_r - \frac{M^2}{L_s}\right)\frac{dI_{rd}}{dt} - \omega_r\left(L_r - \frac{M^2}{L_s}\right)I_{rq} \\ V_{rq} = R_rI_{rq} + \left(L_r - \frac{M^2}{L_s}\right)\frac{dI_{rq}}{dt} + \omega_r\left(L_r - \frac{M^2}{L_s}\right)I_{rd} + \omega_r\frac{M}{L_s}\varphi_s \end{cases} \tag{29}$$

From equations (25), (26) and (27), the synoptic diagram of the DFIG to regulate used the PI regulators.

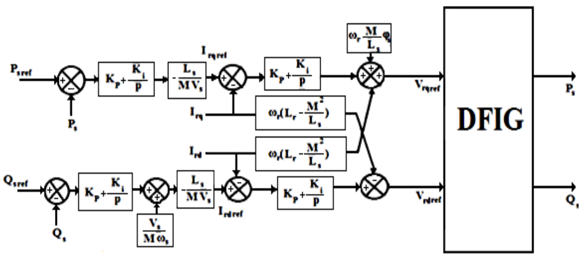

Fig. 3. Vector control indirect for the RSC

C. *DPC for RSC*

Direct power control is analogue to the direct torque control (DTC) introduced for induction motors. The instantaneous active and reactive power are controlled instead of torque and stator flux, (Figure. 4) [14, 22, 23].

The application of the DPC command to the GSC makes it possible in the first place to dispense with the correctors commonly used in order to control a converter. In this command there are no internal loops and eliminates the modulation blocks, it uses only the instantaneous powers as control variable, precisely the errors of the instantaneous powers between the reference values of the instantaneous active and reactive power and their measured values.

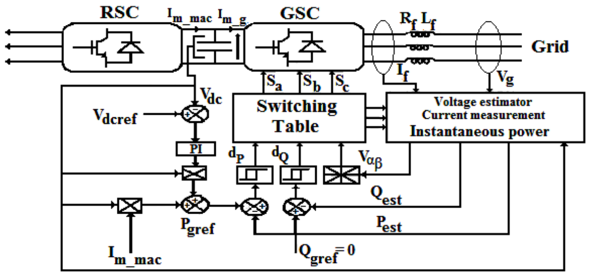

Fig. 4. Direct power control for GSC

Measurement of voltages and currents to determine the value of currents / voltages direct and quadratures using the Concordia transform (α, β) is presented:

$$\begin{bmatrix} I_{f\alpha} \\ I_{f\beta} \end{bmatrix} = \sqrt{\frac{2}{3}} \begin{bmatrix} 1 & -\frac{1}{2} & -\frac{1}{2} \\ 0 & \frac{\sqrt{3}}{2} & -\frac{\sqrt{3}}{2} \end{bmatrix} \quad (30)$$

$$\begin{bmatrix} V_{g\alpha} \\ V_{g\beta} \end{bmatrix} = \sqrt{\frac{2}{3}} \begin{bmatrix} 1 & -\frac{1}{2} & -\frac{1}{2} \\ 0 & \frac{\sqrt{3}}{2} & -\frac{\sqrt{3}}{2} \end{bmatrix} \quad (31)$$

The calculation of instantaneous power without sensors have been assured by estimates the mains voltages from the values of the voltage of the converter and the R_fL_f filter (V-DPC) and establish configurations DPC based on the position of the voltage vector in the stationary α-β reference [23] is given by:

$$\begin{cases} P_{est} = L_f\left(\frac{dI_{ga}}{dt}I_{ga} + \frac{dI_{gb}}{dt}I_{gb} + \frac{dI_{gc}}{dt}I_{gc}\right) + \\ \quad +V_{dc}\left(S_aI_{ga} + S_bI_{gb} + S_cI_{gc}\right) \\ Q_{est} = \frac{1}{\sqrt{3}}\left[3L_f\left(\frac{dI_{ga}}{dt}I_{gc} + \frac{dI_{gc}}{dt}I_{ga}\right) - V_{dc}\{S_a\left(I_{gb} - I_{gc}\right) + \right. \\ \quad \left. +S_b\left(I_{gc} - I_{ga}\right) + S_c\left(I_{gc} - I_{ga}\right)\right] \end{cases} \quad (32)$$

The instantaneous reactive power is compared with the reference reactive power Q_{gref} which is directly imposed at zero to ensure operation with a unit power factor, the instantaneous active power compared to the reference active power Pgref is the addition of the calculated power as a function of the DC-Link voltage at the output of the converter and the power generated by the DFIG, a PI regulator to check the error between the voltage Vdc and the reference Vdcref [21].

The regulators used are hysteresis comparators; in our case we use two regulators at two levels (0 or 1) to calculate the error signal between the reference values and the estimated values of active and reactive power, the output signal d_P and d_Q of the comparators are defined as [15, 23, 24].

$$\begin{cases} d_p = 1 & \Rightarrow & P_{est} \le P_{gref} - H_P \\ d_p = 0 & \Rightarrow & P_{est} \ge P_{gref} - H_P \end{cases} \quad (33)$$

$$\begin{cases} d_Q = 1 & \Rightarrow & Q_{est} \le Q_{gref} - H_Q \\ d_Q = 0 & \Rightarrow & Q_{est} \ge Q_{gref} - H_Q \end{cases} \quad (34)$$

Where: HP and HQ are the hysteresis bands.

θ: The position of the voltage vector in the plan (α, β) can be determined:

$$\theta = tan^{-1}\left(\frac{V_{g\alpha}}{V_{g\beta}}\right) \quad (35)$$

When θ is known, it is necessary to determine in which sector it is for this purpose the plan (α, β) divided into 12 sectors, the sectors can be expressed [15, 23, 24]

$$(n-2)\frac{\pi}{6} \le \theta_n \le (n-1)\frac{\pi}{6}, n = 1 \dots 12 \quad (36)$$

The switching table takes as input the errors dp, dq and the voltage vector position (1 to 12), the switching states Sa, Sb, and Sc of the converter are selected by this switching table; as shown in Table 1 [14, 15].

Table 1 Switching table for DPC

d_P	d_q	θ_1	θ_2	θ_3	θ_4	θ_5	θ_6	θ_7	θ_8	θ_9	θ_{10}	θ_{11}	θ_{12}
1	0	V_6	V_7	V_1	V_0	V_2	V_7	V_3	V_0	V_4	V_7	V_5	V_0
	1	V_7	V_7	V_0	V_0	V_7	V_7	V_0	V_0	V_7	V_7	V_0	V_0
0	0	V_6	V_1	V_1	V_2	V_2	V_3	V_3	V_5	V_4	V_6	V_6	V_1
	1	V_1	V_2	V_2	V_3	V_3	V_4	V_4	V_5	V_4	V_6	V_6	V_1

Where: $V_1(100)$, $V_2(110)$, $V_3(010)$, $V_4(011)$, $V_5(001)$, $V_6(101)$, $V_0(000)$, $V_7(111)$

IV SIMULATION AND ANALYSIS

The simulation of the wind system based on a DFIG illustrated in Figure. 1 is realized with SIMULINK. The parameters used in the simulations are given in the annexes.

Figure 5 shows the example of wind profile applied to the system studied in this article is constructed from the spectral characteristic of Van der Hoven [25]. Its equation is given by:

$$v = 12 + 2\sin\left(2.5t - \frac{\pi}{5}\right) + 2\sin\left(4t - \frac{\pi}{3}\right) + \\ +1.5\sin\left(5.4t - \frac{\pi}{12}\right) + +0.5\sin\left(2.5t - \frac{\pi}{12}\right) \quad (37)$$

The results of adjustment of the mechanical speed is ensured for PI regulator (Figure 6) is represented in the figure, these curve show that the proposed control is very satisfactory, ie the measured speed is identical to the reference obtained through the MPPT control strategy for the controller.

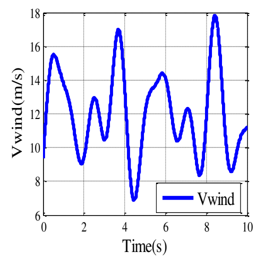

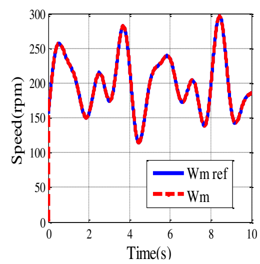

Fig. 5. Wind speed profile. Fig. 6. Speed control of DFIG.

Figure 7 and Figure 8 show the active and reactive stator powers of the DFIG with their references. The reference active stator powers are obtained by the MPPT control. The reference reactive power will be maintained at zero to ensure a unit power factor on the stator side in order to optimize the quality of the energy returned to the grid, we note that the measured active and reactive powers of the DFIG follow their references; this ensures decoupled active and reactive power control of good performances.

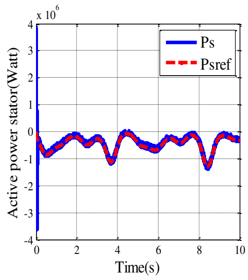

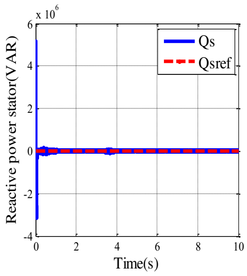

Fig. 7. Stator active power Fig. 8. Stator Reactive power

Figures 9 and 10 show that the quadrature component of the rotor current controls the active power, and the direct component controls the reactive power exchanged between the stator and the grid.

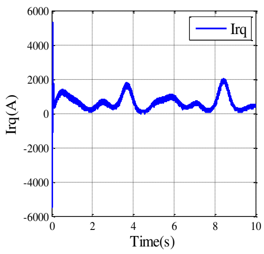

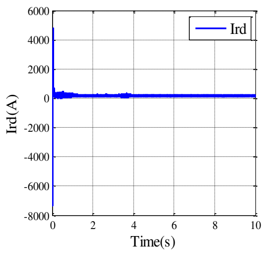

Fig. 9. Rotor current quadrature Fig. 10. Rotor current direct

The result of the DC Link voltage is shown in Figure 11; The DC link voltage reference is set to 1200 V, the measured voltage perfectly follows the reference voltage with the exception of the initial conditions where the voltage control loop does not have enough time to react. This shows the efficiency of the used PI regulator on the control of the DC Link voltage.

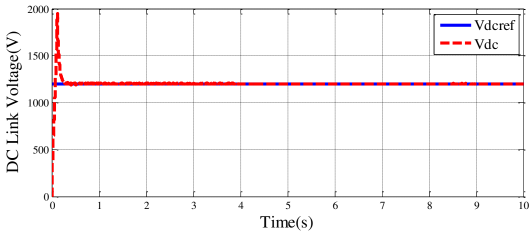

Fig. 11. DC Link Voltage control

Figures 12 and 13 illustrates the evolution of the filter current and the voltage grid, we note that the filter current is in phase with the voltage grid during the period (t = 8.30s to 8.55s) which explains that the rotor of the DFIG absorbs an active power of the grid (hypo-synchronous). However, during the period (t = 8.55s to 8.65s) the filter current is in phase opposition to the voltage grid, so the rotor of the DFIG also provides active power to the grid (hyper-synchronous).

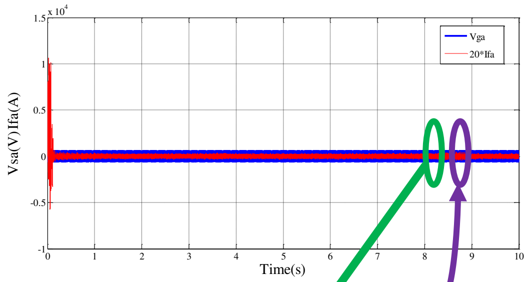

Fig. 12. The voltage grid and the filter current

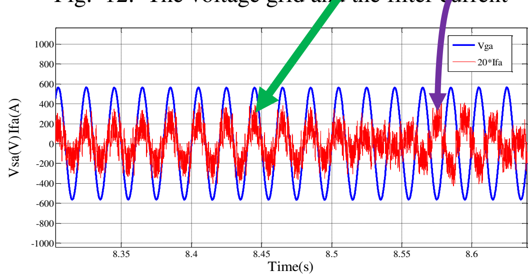

Fig. 13. Zoom the voltage grid and the filter current

V. CONCLUSION

In this article, the system for producing electrical energy based on DFIG variable speed. The MPPT technique with speed control by PI regulator is presented, a control structure combines between VC and DPC has been proposed for the RSC and GSC. This combination will make it possible to take advantage of the two techniques, the VC is very effective for variable speed systems, stable performance, less ripple, it is used for decoupling control of active and reactive powers using indirect flux oriented by means of the PI regulators in order to obtain injected rotor voltages. The DPC with these advantages the simplicity, don't need imbricate loops, and less dependent on the parameters, it uses a switching table to ensures DC Link voltage control using PI and reactive power.

The results of global system simulation such as speed control, indirect active and reactive powers control, DC Link voltage control give very high performances. For the purpose of future extension combined VC, DPC (CVDPC).

ANNEXES

Table 2 DFIG Parameters [19]

Parameters	value
Rated Power	1.5 MW
Stator Voltage	690 V
Stator resistance	0.012 Ω
Rotor resistance	0.021 Ω
Stator inductance	0.0137 H
Rotor inductance	0.0136 H
Mutual inductance	0.0135 H
Moment of inertia	1000 $kg.m^2$
Coefficient of friction	0.0024 $N.m.S^{-1}$
Numbers of pole pairs	2

Table 3 Turbine Parameters [19]

Parameters	value
Rated Power	1.5 MW
Wind turbin Raduis	35.25 m
Gearbox ratio	90

Table 4 Filter Parameters [19]

Parameters	value
Filter Resistance	2 mΩ
Filter Inductance	5 mH
Capacitor of dc link voltage	4400 µF

Table 5 PI Controller Parameters

Parameters	value
DFIG speed controller parameters	Kp=1.64×105 Ki=1.3456×107
Rotor currents Controller parameters	Kp=0.0363 Ki=2.5632
Active and reactive power Controller parameters	Kp=200 Ki=1
DC Link Voltage Controller parameters	Kp=3.5837 Ki=89.3544

REFERENCES

[1] J.Mohammadi, S.Vaez-Zadeh, S.Afsharnia, and E. Daryabeigi, ″A combined vector and direct power control for DFIG-based wind turbines″, In: IEEE Trans Sustain Energy Vol. 29, No .3, pp. 767–775, 2014.

[2] S. Abdeddaim and A. Betka, ″Optimal tracking and robust power control of the DFIG wind turbine″, In: Electrical Power and Energy Systems Vol.49, pp.234–242, 2013.

[3] B. Beltran, T.Ahmed-Ali, and M. El H. Benbouzid, ″Sliding Mode power control of variable speed wind energy conversion systems″, In: IEEE Trans. Energy Conversion, vol. 23, No. 2, pp. 551-558, 2008.

[4] E.G. Shehata and G.M.Salama, ″Direct power control of DFIGs based wind energy generation systems under distorted grid voltage conditions″, In: Electrical Power and Energy Systems Vol.53, pp.956–966, 2013.

[5] V.N. Pande, U.M. Mate, and S. Kurode, ″Discrete sliding mode control strategy for direct real and reactive power regulation of wind driven DFIG″, In: Electric Power Systems Research Vol.100, pp.73– 81, 2013.

[6] D. Chwa, and K.B.Lee, ″Variable Structure Control of the Active and Reactive Powers for a DFIG in Wind Turbines″, In IEEE Transactions on Industry Applications, Vol. 46, No. 6, pp.2545-255, November/December 2010.

[7] S. Li, A. Haskew, K. A.Williams, and R. P. Swatloski, ″Control of DFIG wind turbine with direct-current vector control configuration″, In: IEEE Trans. Sustain. Energy, Vol. 3, No. 1, pp. 1–11, Jan. 2012.

[8] S. Muller, M. Deicke, and R.W.D. Doncker, ″Doubly fed induction generator systems for wind turbines″, In: IEEE Industry Applications Magazine Vol. 8, pp.26–33, 2002.

[9] A. Boyette, S. Saadate, P. Poure, ″Direct and indirect control of a Doubly Fed Induction Generator wind turbine including a storage unit″, In: 32th edition of Industrial Electronics Conference IECON’2006, IEEE, Paris, France, November 6-10, 2006, pp. 2517–2522.

[10] N. Belhaouchet, L. Rahmani, S. Begag, ″A Novel Adaptive HBCC Technique for Three-phase Shunt APF″, In: Electric Power Systems Research Vol. 79, pp. 1097–1104, 2009.

[11] M. Cichowlas, M. Malinowski, P. Kazmierkowski, D.L. Sobczuk, and J. Pou, ″Active filtering function of three-phase PWM boost rectifier under different line voltage conditions″, In: IEEE Trans. on Industrial Electronics, vol. 52, No. 2, pp. 410-419, Apr. 2005.

[12] L. Xu, and P. Cartwright, ″Direct active and reactive power control of DFIG for wind energy generation″, In: IEEE Trans. Energy Convers Vol. 21, pp. 750–758, 2006.

[13] J. Hu, H. Nian, B. Hu, and Y. He, ″Direct active and reactive power regulation of DFIG using sliding-mode control approach″, In: IEEE Trans. Energy Convers Vol. 25, No. 4, pp. 1028–1039, Dec. 2010.

[14] T. Noguchi, H. Tomiki, S. Kondo, and I. Takahashi, ″ Direct Power Control of PWM converter without power-source, voltage sensors″, In: IEEE Trans. on Industrial Application Vol. 34, pp. 473-479, 1998.

[15] M. Malinowski, M.P. Kaźmierkowski, S. Hansen, F. Blaabjerg, and G.D. Marques, ″Virtual Flux Based Direct Power Control of Three-Phase PWM Rectifiers″, In: IEEE Trans. on Industrial Applications Vol. 37, No 4, pp. 1019-1027, 2001.

[16] S. El Aimani, ″Modeling of Various Integrated Wind Turbine Technologies in a Medium Voltage Grid″, PhD Thesis, Ecole Centrale de Lille, 2004.

[17] S. Heier, ″Grid Integration of Wind Energy Conversion Systems. In: John Wiley & Sons, 1998.

[18] S. El aimani, B. Francois, B. Robyns, and F. Minne, ″Modeling and Simulation of Doubly Fed Induction Generators for Variable Speed Wind Turbines Integrated in a Distribution Network″, In: 10th European Conference on Power Electronics and Applications (EPE 2003), Toulouse, France, September 2003.

[19] A. Gaillard, ″Wind system based on the DFIG: contribution to the study of the quality of the electric energy and the continuity of service″, Phd Thesis, Henri Poincare University, Nancy-I, France, April. 2010.

[20] Hamzaoui, F. Bouchafaa, A. Hadjammar, and A. Talha, ″ Improvement of the performances MPPT system of wind generation″, In: Electronics, Communications and Photonics Conference (SIEC 2011) Saudi International, pp. 1-6, 2011.

[21] M. K. Das and al, ″Control of a grid connected doubly-fed induction generators for wind energy conversion″, In: Proceedings of the 44th International Universities Power Engineering Conference (UPEC), pp. 1-5, 2009.

[22] M. Malinowski and P. Kazmierkowski, ″Direct power control of three-phase pwm rectifier using space vector modulation–simulation study″, In: Proc IEEE ISIE’02, Vol. 4, pp. 1114–1118, Jul 2002.

[23] M. Malinowski, M.P. Kazmierkowski, and A. Trzynadlowski, ″Review and comparative study of control techniques for three-phase PWM rectifiers″, In: Mathematics and Computers in Simulation Vol. 63, pp. 349–361, 2003.

[24] M. Malinowski, M. Jasinski, and M.P. Kazmierkowski, ″Simple Direct Power Controlof Three-Phase PWM Rectifier Using Space Vector Modulation″, In: IEEE Transaction Industrial Electronics, Vol. 51, No 2, pp. 447-454, April 2004.

[25] Y. Liu, and J. Wang, ″A Large Time Scale Wind Velocity Simulation Method″, In: International Conference on Computer Design and Applications (ICCDA2010), pp. 282 -286, 2010.